

Giant nonlinearity in a superconducting sub-terahertz metamaterial

V. Savinov,^{1,a)} K. Delfanazari,¹ V. A. Fedotov,¹ and N. I. Zheludev^{1,2}

¹*Optoelectronics Research Centre and Centre for Photonic Metamaterials, University of Southampton, Southampton, SO17 1BJ, United Kingdom*

²*Centre for Disruptive Photonic Technologies, TPI, Nanyang Technological University, Singapore 637371, Singapore*

(Received 1 December 2015; accepted 28 February 2016; published online 10 March 2016)

We report a superconducting sub-THz metamaterial operating in a CW-regime, which exhibits a record-breaking resonant third-order nonlinearity with effective $n_2 \sim 10 \text{ cm}^2/\text{W}$. The nonlinear response is caused by the radiation-induced resistive heating, suppressing the superconductivity in the nano-scale constrictions of the structure's meta-molecules. The nonlinearity has a relaxation time of $25 \mu\text{s}$ and leads to a substantial change of the amplitude and phase of the transmitted radiation at intensities of only $500 \mu\text{W}/\text{cm}^2$. © 2016 AIP Publishing LLC.

[<http://dx.doi.org/10.1063/1.4943649>]

Nonlinear electromagnetic response enables switching light with light and achieving wavelength conversion.¹ Applications of nonlinear optical response include high-speed communications,² sub-wavelength biological imaging,³ and virtually all of modern opto-electronics. Important cubic nonlinearity can be expressed through the complex intensity-dependent refractive index. In case of dielectrics, the nonlinear refractive index is real and lies in the range of $n_2 \sim 10^{-14} - 10^{-16} \text{ cm}^2/\text{W}$.¹ In semiconductors, such as silicone, $n_2 \sim 10^{-14} \text{ cm}^2/\text{W}$.¹ Even stronger nonlinearity occurs in conjugated polymers with $n_2 \sim 10^{-12} \text{ cm}^2/\text{W}$,¹ and graphene with $n_2 \sim 10^{-7} \text{ cm}^2/\text{W}$.⁴ For liquid crystals, $n_2 \sim 10^{-3} \text{ cm}^2/\text{W}$ is accessible, although only at sufficiently long time-scales.¹

Electromagnetic metamaterials are artificial media created by structuring on the scale smaller than the wavelength of the electromagnetic excitation.⁵⁻⁷ The basic building blocks of metamaterials, the meta-molecules, are often designed to be sub-wavelength resonators that trap and confine the energy of the incident radiation. As a result, combining a metamaterial with a suitable natural medium allows to significantly boost the nonlinear response of the latter.

The metamaterials with nonlinear response have now been demonstrated in the spectral ranges starting from microwaves and going up to visible.⁷ A particularly important development has been the demonstration of the nonlinear superconductor- and semiconductor-based metamaterials in the terahertz spectrum⁸⁻¹³ (100 GHz–30 THz (Ref. 14)), where most natural media do not exhibit significant nonlinearities.¹⁵ Recently, it was shown that the superconducting terahertz metamaterials exhibit substantial nonlinearity related to the suppression of superconductivity by pulsed radiation with the peak intensities exceeding $2 \times 10^3 \text{ W}/\text{cm}^2$.^{10-12,16} Here, we will demonstrate a sub-THz superconducting metamaterial with nonlinearity that corresponds to effective $n_2 \sim 10 \text{ cm}^2/\text{W}$ and is accessible with CW-excitation at intensities below $10^{-3} \text{ W}/\text{cm}^2$.

Before proceeding, we will briefly overview the properties that make the superconducting metamaterials particularly

well-suited for operation at frequencies up to and including terahertz.¹⁷ The superconducting metamaterials offer low Joule losses, sub-nanosecond nonlinear response,¹⁸⁻²⁰ access to quantum-mechanical phenomena through the inclusion of Josephson junctions,²¹⁻²³ and sensitivity to light,²⁴ magnetic field, and temperature.^{7,25,26} The nonlinear response of the superconductors at terahertz/sub-THz frequencies occurs via two mechanisms. First, large oscillating currents can heat the superconductor, thus increasing its resistance.²⁷ Second, through the induced magnetic fields, large currents can lead to the sub-nanosecond scale break-up of the Cooper pairs, the carriers of low-loss currents in superconductors,^{10-12,18,19,27-29} which will also increase the resistance.

In this paper, we show that the radiation-induced resistive heating, suppressing the superconductivity in a metamaterial array, the first mechanism of nonlinear response, can become a source of strong and fast nonlinearity. The strong nonlinear response is achieved by confining the radiation-induced current in specially designed nano-scale constrictions, leading to large current densities, as shown in Fig. 1. The large current densities suppress superconductivity in the constrictions, thus giving rise to the nonlinear response. The small size of constrictions ensures that heating is strongly localized, which also allows for microsecond cooling times, thus offering a fast nonlinear response.

Figures 1(b) and 1(c) show our metamaterial a two dimensional array of superconducting asymmetrically split ring meta-molecules ($550 \mu\text{m} \times 550 \mu\text{m}$) on a dielectric substrate. This metamaterial has been extensively studied in microwave,³⁰ terahertz,³¹⁻³⁵ and optical ranges.³⁶ The size of the unit-cell is dictated by the substrate permittivity and the target resonant frequency, the asymmetry of the splits in the rings controls the quality factor of metamaterial response. The geometry of the unit cell in this paper is based on our previous work.^{33,34} In the meta-molecules, the width of the superconducting arcs was $30 \mu\text{m}$. It narrowed down to just $3 \mu\text{m}$ at the mid-points of the arcs. At resonance, the maxima of the currents, induced in the metamaterial by the incident radiation, occur at the mid-points of the arcs;³⁰ therefore, placing constrictions at these points allows to achieve a maximum current density. The metamaterial was manufactured in two stages. In

^{a)}vs1106@orc.soton.ac.uk

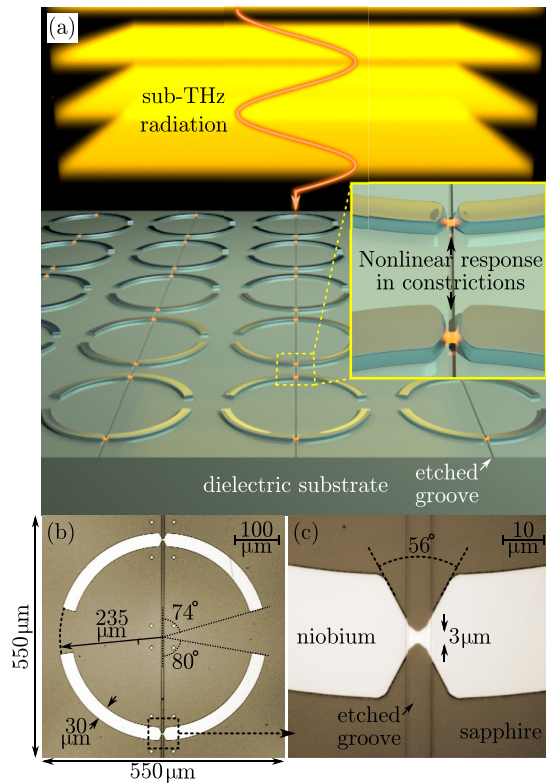


FIG. 1. Design of the metamaterial. (a) Artistic illustration of metamaterial's operation. The incident radiation induces currents in the metamaterial, an array of superconducting asymmetrically split rings on a dielectric substrate. Each ring contains two constrictions at points of maximum current amplitude. The current density is enhanced at the constrictions, which engages the nonlinear response of the superconductor. (b) and (c) The microscope pictures of the metamaterial unit cell. Lighter areas are the niobium film (300 nm thick), and the darker areas are the sapphire substrate (0.5 mm thick).

the first stage, a 300 nm niobium film on the sapphire substrate (0.5 mm thick) was photo-lithographically patterned to create the base structure. In the second photo-lithography stage, a narrow groove was etched into each meta-molecule along the symmetry axis, leaving constrictions of thickness 80 nm. In both cases, ion beam milling was used to etch the niobium film.

The metamaterial sample was housed inside an optical cryostat and its transmission was measured at a normal incidence with the radiation intensity below $100 \mu\text{W}/\text{cm}^2$.³⁷ The transmission spectrum is shown in Fig. 2(a). At temperatures below $\theta_c \approx 9 \text{ K}$, niobium enters the superconducting state characterized by a low sub-THz resistivity with a strong dependence on the temperature.³⁸ At lowest attainable temperature, $\theta \approx 4 \text{ K}$, our metamaterial displayed an asymmetrically shaped transmission peak around $\nu = 97.4 \text{ GHz}$, which is known as the trapped mode resonance.^{30,31,33,34,39,40} It is created by the anti-symmetric current oscillations in the two arcs of each meta-molecule, which leads to the suppression of the net radiation scattered by the metamaterial and thus to a peak in transmission. Increasing the metamaterial temperature, from 4 K towards θ_c , causes a rapid increase in the Joule losses, which, in turn, results in the suppression of the trapped mode. Above the critical temperature ($\theta_c \approx 9 \text{ K}$), niobium enters the

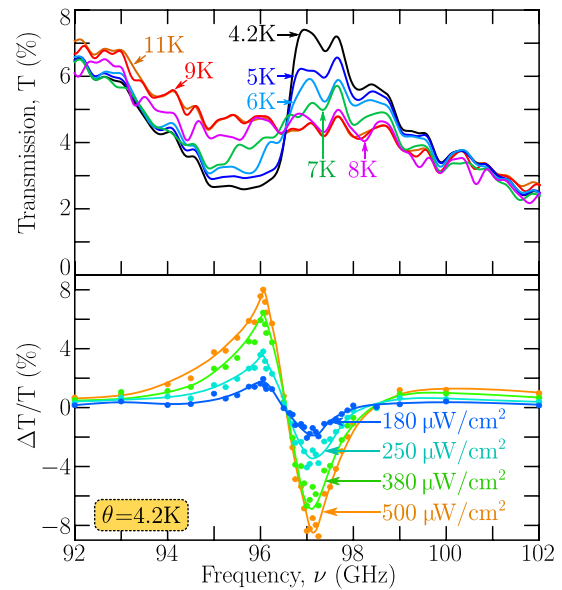


FIG. 2. Metamaterial transmission spectrum. (a) Metamaterial transmission measured with radiation intensity below $100 \mu\text{W}/\text{cm}^2$. Different curves correspond to different substrate temperatures. Fringes in the transmission are caused by spurious reflections inside the cryostat as well as by small oscillations of metamaterial temperature during the frequency sweep. (b) The difference in the metamaterial transmission when measured at a high radiation intensity ($I_0 = 112 \mu\text{W}/\text{cm}^2$) compared to measurement at a low radiation intensity ($I_0 = 112 \mu\text{W}/\text{cm}^2$). All measurements have been carried out at temperature $\theta = 4.2 \text{ K}$.

normal state, and the asymmetric transmission peak effectively vanishes from the metamaterial transmission spectrum.

The level of peak transmission at the trapped mode resonance in our metamaterial reaches 7.4% (11 dB insertion loss; see Fig. 2(a)); however, the insertion loss here is of non-resonant nature and can be lowered in a number of ways.³⁷ This will enable stacking the metamaterials.

Measuring the metamaterial transmission with radiation intensities above $100 \mu\text{W}/\text{cm}^2$ revealed a nonlinear response.³⁷ Figure 2(b) shows the intensity-dependent difference in the metamaterial transmission (at $\theta \approx 4.2 \text{ K}$), for several representative radiation intensities. The metamaterial transmission exhibited a strong dependence on the intensity of incident radiation around the trapped mode resonance. At frequencies below 96.5 GHz, the transmission increased in response to the increasing intensity, whilst at frequencies above 96.5 GHz, the transmission decreased.

To confirm that the observed difference in the metamaterial transmission resulted from the suppression of the superconducting state, the transmission was measured at a fixed frequency 97 GHz as a function of temperature. The relative difference in transmission, shown in Fig. 3(a), appeared only at low temperatures, reaching almost -10% at temperature $\theta = 4 \text{ K}$ and at a radiation intensity of $500 \mu\text{W}/\text{cm}^2$. We therefore argue that the nonlinear response of the metamaterial was related to the suppression of superconductivity.

Figure 3(b) shows the intensity-dependent phase difference in the metamaterial transmission when measured at an intensity of $500 \mu\text{W}/\text{cm}^2$ and at an intensity of $112 \mu\text{W}/\text{cm}^2$. As in Fig. 3(a), the nonlinear response appears only below the

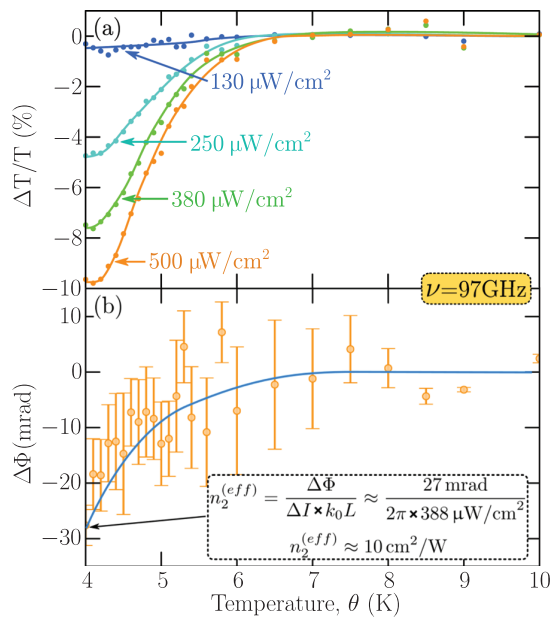


FIG. 3. Metamaterial nonlinear response at $\nu = 97$ GHz as a function of temperature. (a) The difference in the metamaterial transmission measured at a high radiation intensity ($500 \mu\text{W}/\text{cm}^2$) compared to measurement at a low radiation intensity ($I_0 = 112 \mu\text{W}/\text{cm}^2$). For example, the curve labeled $500 \mu\text{W}/\text{cm}^2$ shows that at temperature 4 K, the metamaterial transmission at the intensity $500 \mu\text{W}/\text{cm}^2$ will be 10% lower than the transmission at the intensity I_0 . (b) Phase difference of the metamaterial transmission measured at a radiation intensity of $500 \mu\text{W}/\text{cm}^2$ compared to measurement at the intensity I_0 , as a function of temperature. The data show the intensity-dependent transmission phase delay, which can be used to estimate the real part of the second-order refractive index n_2 (inset).

critical temperature of niobium and is strengthened when the temperature is further reduced. One can use the nonlinear phase delay ($\Delta\Phi$) to estimate the real part of the effective second-order refractive index of the metamaterial $n_2^{(eff)} = \Delta\Phi/k_0L\Delta I$, where k_0 is the free-space radiation wavenumber, L is the thickness of the medium, and ΔI is the difference in radiation intensity. The total thickness of the metamaterial, including the substrate, is only 0.5 mm, i.e., about six times smaller than the free-space wavelength of the incident radiation ($c/97 \text{ GHz} \approx 3.1 \text{ mm}$). For the purpose of conservative estimate of the nonlinearity, we will assume metamaterial thickness equal to the free-space wavelength, which results in $n_2^{(eff)} \approx 10 \text{ cm}^2/\text{W}$; equivalently, the surface nonlinear refractive index is $n_2^{(surface)} = \Delta\Phi/k_0\Delta I \approx 3 \text{ cm}/\text{W}$.

The large current densities, forced through the constrictions in the split-ring resonators of our metamaterial, can give rise to nonlinear response either by heating the niobium or by splitting the superconducting charge carriers, the Cooper pairs, with large magnetic fields. Our analysis shows that for niobium on the sapphire substrate, such as in our experiments, the nonlinearity due to heating will dominate unless the radiation is supplied in short pulses.³⁷ The characteristic cooling down time for niobium on the sapphire substrate is $25 \mu\text{s}$ (Ref. 33)—the relaxation time for the thermal nonlinearity.

Faster nonlinear response, with the relaxation time shorter than 1 ns, will occur when the current induced in the metamaterial will exceed the critical current of the small

constrictions (14 mA). According to our analysis,³⁷ this can be achieved at the CW-intensity level of about $200 \text{ mW}/\text{cm}^2$ or, in the pulse regime with sub-nanosecond pulses at $100 \text{ pJ}/\text{cm}^2$ fluence. By comparison, all previously demonstrated nonlinear THz metamaterials operated in the fluence range of $1 - 100 \text{ nJ}/\text{cm}^2$ ^{10–12} or even higher.

In conclusion, we have demonstrated a superconducting sub-THz metamaterial, which, through nano-scale engineering of current constrictions, allows to achieve the nonlinear response with $n_2^{(eff)} \sim 10 \text{ cm}^2/\text{W}$. The transmission change of almost 10% has been demonstrated with the radiation intensity of only $500 \mu\text{W}/\text{cm}^2$. Using the experimental data and a realistic heat transfer model, we estimate that the nonlinear response with sub-nanosecond relaxation times shall be observed at radiation intensities of only $200 \text{ mW}/\text{cm}^2$. The principle behind the metamaterial operation can be extended into the THz-range using niobium and high- T_c superconductors. The proposed type of nonlinear metamaterials could be used in applications such as switching, routing, heterodyne detection, dynamic image processing, image recognition, holography, and 2D adaptive filtering of the THz and sub-THz frequencies, complementing solutions based on semiconductor electronics.

This study was supported by the Engineering and Physical Sciences Research Council (Grant Nos. EP/G060363/1 and EP/M009122/1), the Royal Society, and the Singapore Ministry of Education (Grant No. MOE2011-T3-1-005). The data from this paper can be obtained from the University of Southampton ePrints repository: <http://dx.doi.org/10.5258/SOTON/384516>.

¹R. W. Boyd, *Nonlinear Optics* (Academic Press, 2008).

²D. Cotter, R. J. Manning, K. J. Blow, A. D. Ellis, A. E. Kelly, D. Nessel, I. D. Phillips, A. J. Poustie, and D. C. Rogers, *Science* **286**, 1523 (1999).

³W. R. Zipfel, R. M. Williams, and W. W. Webb, *Nat. Biotechnol.* **21**, 1369 (2003).

⁴H. Zhang, S. Virally, Q. Bao, L. K. Ping, S. Massar, N. Godbout, and P. Kockaert, *Opt. Lett.* **37**, 1856 (2012).

⁵N. I. Zheludev, *Science* **328**, 582 (2010).

⁶C. M. Soukoulis and M. Wegener, *Nat. Photonics* **5**, 523 (2011).

⁷N. I. Zheludev and Yu. S. Kivshar, *Nat. Mater.* **11**, 917 (2012).

⁸M. Liu, H. Y. Hwang, H. Tao, A. C. Strikwerda, K. Fan, G. R. Keiser, A. J. Sternbach, K. G. West, S. Kittiwatanakul, J. Lu, S. A. Wolf, F. G. Omenetto, X. Zhang, K. A. Nelson, and R. D. Averitt, *Nature* **487**, 345 (2012).

⁹K. Fan, H. Y. Hwang, M. Liu, A. C. Strikwerda, A. Sternbach, J. Zhang, X. Zhao, X. Zhang, K. A. Nelson, and R. D. Averitt, *Phys. Rev. Lett.* **110**, 217404 (2013).

¹⁰C. Zhang, B. Jin, J. Han, I. Kawayama, H. Murakami, X. Jia, L. Liang, L. Kang, J. Chen, P. Wu, and M. Tonouchi, *New J. Phys.* **15**, 055017 (2013).

¹¹N. K. Grady, B. G. Perkins, Jr., H. Y. Hwang, N. C. Brandt, D. Torchinsky, R. Singh, L. Yan, D. Trugman, S. A. Trugman, Q. X. Jia, A. J. Taylor, K. A. Nelson, and H.-T. Chen, *New J. Phys.* **15**, 105016 (2013).

¹²C. Zhang, B. Jin, J. Han, I. Kawayama, H. Murakami, J. Wu, L. Kang, J. Chen, P. Wu, and M. Tonouchi, *Appl. Phys. Lett.* **102**, 081121 (2013).

¹³İ. Al-Naib, G. Sharma, M. M. Dignam, H. Hafez, A. Ibrahim, D. G. Cooke, T. Ozaki, and R. Morandotti, *Phys. Rev. B* **88**, 195203 (2013).

¹⁴M. Tonouchi, *Nat. Photonics* **1**, 97 (2007).

¹⁵K. Tanaka, H. Hirori, and M. Nagai, *IEEE Trans. Terahertz Sci. Technol.* **1**, 301 (2011).

¹⁶J. Wu, C. Zhang, L. Liang, B. Jin, I. Kawayama, H. Murakami, L. Kang, W. Xu, H. Wang, J. Chen, M. Tonouchi, and P. Wu, *Appl. Phys. Lett.* **105**, 162602 (2014).

¹⁷R. Singh and N. I. Zheludev, *Nat. Photonics* **8**, 679 (2014).

¹⁸M. D. Sherrill and K. Rose, *Rev. Mod. Phys.* **36**, 312 (1964).

¹⁹C. C. Chin, D. E. Oates, G. Dresselhaus, and M. S. Dresselhaus, *Phys. Rev. B* **45**, 4788 (1992).

- ²⁰C. Zhang, B. Jin, A. Glossner, L. Kang, J. Chen, I. Kawayama, H. Murakami, P. Müller, P. Wu, and M. Tonouchi, *J. Infrared, Millimeter, Terahertz Waves* **33**, 1071 (2012).
- ²¹M. Trepanier, D. Zhang, O. Mukhanov, and S. M. Anlage, *Phys. Rev. X* **3**, 041029 (2013).
- ²²S. Butz, P. Jung, L. V. Filippenko, V. P. Koshelets, and A. V. Ustinov, *Opt. Express* **21**, 22540 (2013).
- ²³P. Jung, S. Butz, M. Marthaler, M. V. Fistul, J. Leppäkangas, V. P. Koshelets, and A. V. Ustinov, *Nat. Commun.* **5**, 3730 (2014).
- ²⁴R. Singh, J. Xiong, A. K. Azad, H. Yang, S. A. Trugman, Q. X. Jia, A. J. Taylor, and H.-T. Chen, *Nanophotonics* **1**, 117 (2012).
- ²⁵S. M. Anlage, *J. Opt.* **13**, 024001 (2011).
- ²⁶W. Cao, R. Singh, C. Zhang, J. Han, M. Tonouchi, and W. Zhang, *Appl. Phys. Lett.* **103**, 101106 (2013).
- ²⁷C. Kurter, A. P. Zhuravel, A. V. Ustinov, and S. M. Anlage, *Phys. Rev. B* **84**, 104515 (2011).
- ²⁸M. A. Golosovsky, H. J. Snortland, and M. R. Beasley, *Phys. Rev. B* **51**, 6462 (1995).
- ²⁹C. Kurter, P. Tassin, A. P. Zhuravel, L. Zhang, T. Koschny, A. V. Ustinov, C. M. Soukoulis, and S. M. Anlage, *Appl. Phys. Lett.* **100**, 121906 (2012).
- ³⁰V. A. Fedotov, M. Rose, S. L. Prosvirnin, N. Papasimakis, and N. I. Zheludev, *Phys. Rev. Lett.* **99**, 147401 (2007).
- ³¹V. A. Fedotov, A. Tsiatmas, J. H. Shi, R. Buckingham, P. A. J. de Groot, Y. Chen, S. Wang, and N. I. Zheludev, *Opt. Express* **18**, 9015 (2010).
- ³²R. Singh, I. A. I. Al-Naib, M. Koch, and W. Zhang, *Opt. Express* **19**, 6312 (2011).
- ³³V. Savinov, V. A. Fedotov, S. M. Anlage, P. A. J. de Groot, and N. I. Zheludev, *Phys. Rev. Lett.* **109**, 243904 (2012).
- ³⁴V. Savinov, V. A. Fedotov, P. A. J. de Groot, and N. I. Zheludev, *Supercond. Sci. Technol.* **26**, 084001 (2013).
- ³⁵V. A. Fedotov, J. Wallauer, M. Walther, M. Perino, N. Papasimakis, and N. I. Zheludev, *Light Sci. Appl.* **4**, e306 (2015).
- ³⁶V. A. Fedotov, T. Uchino, and J. Y. Ou, *Opt. Express* **20**, 9545 (2012).
- ³⁷See supplementary material at <http://dx.doi.org/10.1063/1.4943649> for further experimental/numerical details.
- ³⁸A. A. V. Pronin, M. Dressel, A. Pimenov, A. Loidl, I. V. Roshchin, and L. H. Greene, *Phys. Rev. B* **57**, 14416 (1998).
- ³⁹N. I. Zheludev, S. L. Prosvirnin, N. Papasimakis, and V. A. Fedotov, *Nat. Photonics* **2**, 351 (2008).
- ⁴⁰B. Luk'yanchuk, N. I. Zheludev, S. A. Maier, N. J. Halas, P. Nordlander, H. Giessen, and C. T. Chong, *Nat. Mater.* **9**, 707 (2010).